

Short Communication

Chemical Deposition of ITO/CdS/PbS/C for Low Voltage Photosensor Applications

C.E. Pérez-García, S. Meraz-Dávila, E.A. Chávez-Urbiola, I.R. Chávez-Urbiola*,
F. Willars-Rodríguez, R. Ramírez-Bon, Y. Vorobiev

Centro de Investigación y de Estudios Avanzados del IPN. Unidad Querétaro Apdo. Postal 1-798,
76001, Querétaro, Qro., México.

*Texas Materials Institute, The University of Texas, Austin, Texas 78712

*E-mail: rrbon@cinvestav.mx

Received: 13 November 2017 / Accepted: 12 January 2018 / Published: 6 March 2018

In this work we report the assembling and electrical characterization of ITO/CdS/PbS/C heterostructured photosensor. The assembling of the photosensor was done completely by solution processing, employing the chemical bath deposition (CBD) technique to deposit both semiconductor layers in the device, CdS and PbS. ITO-coated glass was used as substrate and graphite ink electrodes as back contacts. The electrical output response of the photodevices was analyzed in dark and under illumination at different intensities. Its sensitivity was examined working as photodiode at zero volts. The results showed the rectifying character of the heterostructure and light sensitivity with linear photoresponse under illumination. The measured photoresponsivity of the photosensor was 1.22 A/W, which is around 50 % of an ideal characteristic of a sensor for a given spectral range.

Keywords: photosensors; hybrid photodiodes; solution growth; chemical deposition.

1. INTRODUCTION

Every year the technological gadgets become more powerful and faster due to the advances in the new electronic components included in them such as transistors, diodes, sensors, etc. These advances are related with the large amount of research on processing and characterization of semiconductor materials to optimize their properties for a wide variety of technological applications. One of the main applications of semiconductor materials is the photovoltaic conversion to generate energy from sunlight by means of thin film solar cells. In this aspect, the current semiconductor photovoltaic technologies are still far to achieve the theoretical solar cell maximum efficiency for a single p-n junction (33.7%) given by the Shockley-Queisser limit [1]. According to this, the maximum

theoretical efficiency of solar cells can be reached with semiconductor materials with energy band gap around 1.34 eV, decreasing in solar cells with semiconductors with either higher or lower energy band gap. Lead chalcogenides are compound semiconductor materials with energy band gap lower than 1 eV, so the expected performance in solar cell is poor in comparison with other semiconductor materials. However, this issue has not discouraged the research on heterostructures based on lead chalcogenides for solar cells applications. For example, there is still a great interest on thin film solar cells based on the CdS-PbS heterostructure. According with H. Mohamed [2] this heterostructure can reach a maximum theoretical efficiency of 4.13% and experimental works shows an efficiency of 1.63% [3]; the efficiency can be improved by modifying the grain size until they can be treated as quantum dots, as a result the band gap will increase and therefore the efficiency can increase up to 3.3% [4].

The application of p-n heterojunctions for the detection of light with photodiode devices is another important option to apply semiconductor materials, which has been much less studied. It is well known that photodiodes have enhanced photosensitivity when operate at reverse bias. Even at zero volts, due to the photovoltaic effect, photodiodes have the capability to detect light by measuring the short circuit current. This way we can obtain a photo sensor with an operation voltage of 0 volts, which is very important for low energy consumption applications. The spectral response of the photosensors depend on the energy band gaps of the semiconductor layers in the heterostructure, mainly that of the absorbent one. Lead sulfide (PbS) is a low energy band gap semiconductor material with properties for a lot of applications, including photosensors. One of the main advantages of this material is its solution processability by means of CBD. This is a simple, convenient and cost-effective deposition technique to obtain nanocrystalline PbS thin films [5, 6]. In our group we have developed PbS thin films deposited by CBD and successfully applied them in thin film solar cells and thin film transistors [7]. In this work we assembled CdS-PbS heterostructures on ITO-coated glass substrates employing the CBD technique for the deposition of both semiconductor layers. The CdS and PbS films were deposited at 70 °C and room temperature (25°C), respectively employing ammonia-free solutions. No additional thermal treatments were performed on the semiconductor layers. As back contacts, graphite ink electrodes were painted on the PbS layer. We report here the main characteristics of the electrical photoresponse of the Glass/ITO/CdS/PbS/C photodiodes assembled completely in solution at low temperature.

2. EXPERIMENTAL DETAILS

The scheme of the assembled CdS-PbS heterostructure is shown in Fig. 1a). The layers were deposited in sequence, starting with the CdS films, which were grown by CBD on ITO-coated glass substrates with 1x1 inches dimensions. For this, the substrates were immersed vertically in a 100-ml beaker containing the following reaction solution: 15 ml CdCl₂ (0.05M); 15 ml Na citrate (0.5M); 15 ml KOH (0.5M), 5ml pH10 buffer and completed with deionized water. The beaker was placed in a thermal bath at 70 °C and the substrates with the CdS layer were removed after 60 minutes [8, 9]. See for details our proceeding deposition [10, 11] or other reports about PbS synthesis [12–17].

Subsequently, the PbS films were deposited on the Glass/ITO/CdS substrates by immersion in 100 ml beaker with the reaction solution of: 5 ml $\text{Pb}(\text{C}_2\text{H}_3\text{O}_2)_2$ (0.5M); 5ml NaOH (2M); 6 ml $\text{CS}(\text{NH}_2)_2$ (1M); 2ml Triethanolamine (1M) and the volume was completed with deionized water. The deposition process was realized in darkness at room temperature, then, the substrate was removed after 180 min. Finally, ohmic contacts were deposited upon the PbS film using a graphite conductive paint and drying in a furnace at 60 °C for 5 hours. X-Ray diffraction (XRD) patterns of the films were recorded in a Rigaku D/MAX-2000 diffractometer, using a Cu-K α radiation for the CdS films and a Co- K α radiation for the PbS ones. The Current-Voltage (I-V) curves of the assembled photosensors, in dark under variable illumination, were recorded with a semiconductor parameters analyzer Keithley model 4200-SCS. A commercial tungsten-halogen lamp was used as the illumination source. Transient photocurrents were measured using a 2401 Source Meter Keithley Instrument, exciting with pulses of light with 20, 40, 60, 80 and 100 mW/cm² intensity

3. RESULTS AND DISCUSSION

X-ray diffraction (XRD) patterns of both types of chemically deposited films are shown in Fig. 1 b) and c). At the top, the pattern of the PbS film displays diffraction peaks which completely matches with the pattern of the Galena phase of PbS (PDF 05-0592). Meanwhile, the diffraction peaks in the pattern of CdS films corresponds to those of the hexagonal crystalline phase of CdS (PDF 41-1049, CdS Greenockite). The PbS diffraction peaks evidence the polycrystalline nature of the films, with some preferred crystalline orientation along the (200) direction. On the other hand, the cadmium sulfide films have preferential orientation along the (002) orientation, according to the high intensity of the (002) diffraction peak. This crystalline characteristic is typical of chemically deposited CdS films obtained from the ammonia-free, cadmium-citrate system CBD formulation [8, 9].

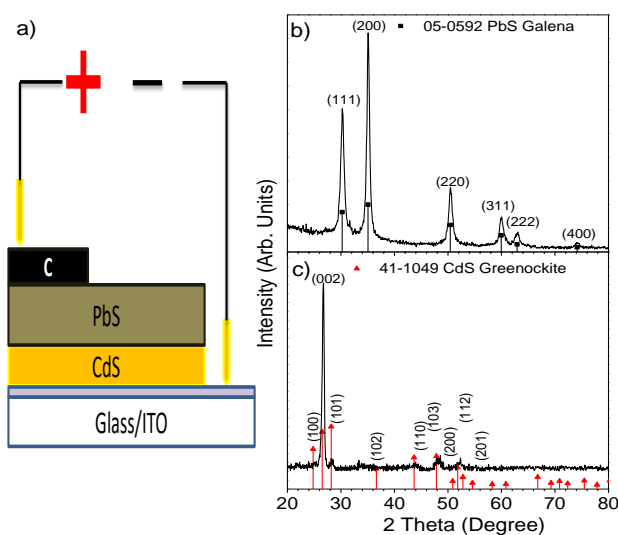


Figure 1. a) Scheme of the Glass/ITO/CdS/PbS/C device layers configuration and X-Ray Diffraction patterns of b) lead sulphide and c) cadmium sulphide layers.

These results show that both films in the device are polycrystalline, the lead sulphide layer presents a cubical structure (Galena) with a lattice parameter $a=5.93 \text{ \AA}$ and the cadmium sulphide layer has a hexagonal structure with lattice parameters $a=4.14 \text{ \AA}$ and $c=6.71 \text{ \AA}$. It is noteworthy that the lead sulphide layer grown on cadmium sulphide is not an epitaxial layer due to the difference of lattice parameters, crystalline structure and polycrystalline nature of cadmium sulphide layer.

The current density versus voltage (J - V) characteristics of the Glass/ITO/CdS/PbS/C photodiodes were measured under dark and various illumination intensities from 0 to 100 mW/cm^2 with intensity steps of 20 mW/cm^2 . The results are shown in Fig. 2 a), where the J - V curves are plotted in semi-log scales. These measurements show the typical rectifying behaviour of a diode with electrical response modified by the incident radiation. The lowest part of the J - V curves shifts to higher voltage as the illumination intensity increases, due to the photovoltaic effect [10, 18, 19]. Therefore, at zero voltage the short circuit current, J_{SC} , due to the photovoltaic effect is determined. The values of J_{SC} changes from 1.37, 66, 92, 114, 140 and 164 mA/cm^2 for 0, 20, 40, 60, 80 and 100 mW/cm^2 , respectively. That is, as expected in a photodiode device, the current density at zero volts increases as incident illumination increases. The current density, at zero volts, increases 3 orders of magnitude, something that does not happen at any other applied voltage. Under illumination, the photogenerated electron-hole pairs are separated more effective at zero voltage than either at forward bias or reverse bias. This observation is based on the sensitivity showed at zero voltage (Fig. 2b).

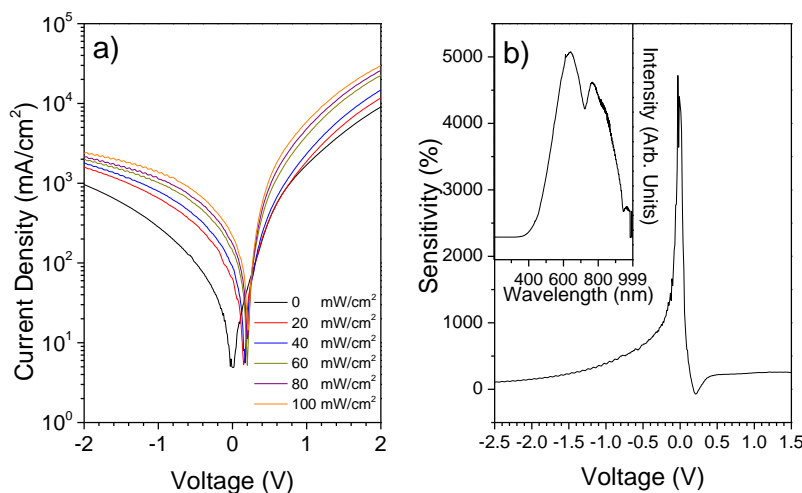


Figure 2. a) Current density-voltage characteristics of the Glass/ITO/CdS/PbS/C photodiode in dark and under illumination at different intensities and b) Photosensitivity versus applied voltage of the CdS/PbS photodiode. The inset shows the radiation spectra of the source light

The photosensitivity usually is obtained by a simple relation between the dark current and photocurrent:

$$S = \frac{I_{ph} - I_d}{I_d} \times 100 \tag{1}$$

where I_d is the dark current and I_{ph} is the photocurrent. This method is used by several authors [20–26]. The dark current is the electrical current measured when the device is in dark and the

photocurrent is the current when the device is illuminated. The photosensitivity as a function of the applied voltage of the Glass/ITO/CdS/PbS/C photodiode is shown in Fig. 2b). In this case the illumination source was a tungsten-halogen lamp at 100 mW/cm^2 intensity (the inset in Fig. 2 b) displays the emission spectrum of this light source). The photosensitivity has a narrow peak at zero volts and decreases at reverse and forward bias. In the -1 to $+1$ volts range, it is observed clearly the typical photodiode behavior with higher photosensitivity at reverse bias than at forward bias. Therefore, it can be taken advantage on the photovoltaic effect produced by the CdS-PbS heterostructure to detect light with high photosensitivity with a device working at zero volts. It is not necessary to apply any voltage because the device can supply electrical current by itself from the incident irradiation.

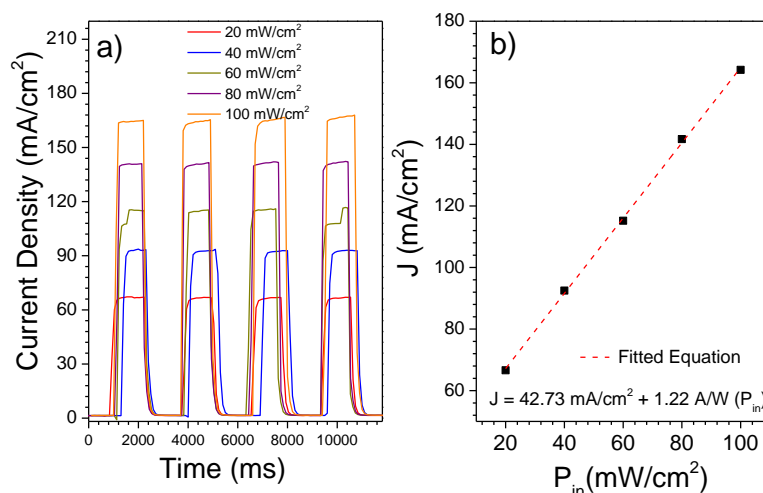


Figure 3. a) Transient photocurrent measurements of the photodiode as a function of illumination intensity and b) Output current density of the photodiode as a function of pulsed light illumination intensity.

The photodetection capability of the Glass/ITO/CdS/PbS/C photodiode was also measured by the light On/Off method. For this, no potential voltage was applied to the device (0 V), meanwhile light pulses produced with the same halogen-tungsten lamp impinged on the heterostructure, and the changes of current density against time were recorded. This procedure is better known as transient photocurrent measurements. We observe in Fig. 3 a) the proper on/off response of the photodiode, the current density increases when the light is turned on, and when it is turned off it drops to its original value. When the device is illuminated (light on), the number of free charge carriers increases producing a photocurrent in excess, which is appreciated as the sudden increase in the current density. While the illumination on the device is maintained, the current density remains constant until the light is turned off when it abruptly decreases to its previous value. In this case, the decrease in the current density is due to the recombination of the photogenerated charge carriers. It is observed that the photocurrent increases with illumination intensity in a linear way as it is shown in Fig. 3 b), where is plotted the photocurrent as a function of light illumination intensity. This is the calibration curve for the CdS-PbS photodiode and can be used to determine its sensitivity as light sensor. The data fit very well to a straight line (dashed line in the graph) with slope 1.22 A/W , which is the photoresponsivity of

the device, that is, the output current of the photodiode per watt of incident light. The photoresponsivity of the device is a useful figure of merit to determine the device performance and to make comparisons with other similar photodevices. These results show the capability and sensitivity of the CdS-PbS heterojunction to work as light sensor at zero volts.

By using the photoresponsivity as figure of merit we can conclude that 1.22 A/W of the CdS-PbS photodiodes is a rather high value as compared with other inorganic or hybrid photodevices.

For example, inorganic heterostructured photodevices have shown photoresponsivity of ZnO/Si 0.34 A/W at -2 V [27], ITO/p-GaN 0.04 A/W at -5 V [28], p-Si/GaN 29 mA/W at -4 V [29], ZnO / Si 0.5 A/W at -4 V [26], ZnO / n-Si 3.06 A/W at -20 V [30], ZnO / n-Si 0.11 A/W at -5 V [41], n-ZnO/p-Si 1.8 A/W [34]. On the other hand, for organic and hybrids photodevices the following photoresponsivity values were found: PEDOT:PSS/P3HT:PCBM 310 mA/W at -2 V [34], PbS QDs:P3HT:PC₆₁BMBH 160 mA/W at -5 V [36], PEDOT:PSS/PbS:P3HT:PCBM 177 mA/W at -1 V [33], Spiro-TDP:CdSe 130-500 mA/W at -5 V [34]. It should be noticed that all these photodevices works in reverse bias with a functional value of applied voltage.

The responsivity is another photosensor property which is a function of the wavelength of the incident radiation. A simple expression for the responsivity, R , which is related with the amount of energy from the optical source that is converted into an electric current is [40,41]:

$$R = \eta \frac{q}{hf} \approx \eta \frac{\lambda(\mu\text{m})}{1.23985 (\mu\text{m} \times \frac{\text{W}}{\text{A}})} \quad (2)$$

where η is the quantum efficiency, q is the fundamental electric charge, h is the Planck's constant, f and λ are the frequency and wavelength of the optical signal. R has units of amperes per watt. Thus, for the case of PbS we can use $\lambda=3 \mu\text{m}$ (corresponding to its band gap of 0.4 eV), and for $\eta=1$ (maximum efficiency) we get $R = 2.42 \text{ A/W}$. Therefore, our photodiodes have about 50% of the maximum possible photoresponsivity

4. CONCLUSIONS

The Glass/ITO/CdS/PbS/C photosensor was achieved successfully by a simple and cheap technology based on the chemical bath deposition of both semiconductor layers in the device. The advantages of this technique include simplicity, low cost and easy reproducibility with no need of special equipment. The characteristics of the photosensor working at zero applied voltage show a higher sensitive at 0 V than in reverse bias, a proper on/off behavior under illumination with a linear dependence on the radiation intensity. The measured photoresponsivity was 1.22 A/W, value which is comparable and even higher to other values reported in literature for similar heterostructured photosensors working in reverse bias. The photosensor reached the half of the theoretical maximum photoresponsivity.

ACKNOWLEDGEMENTS

The technical assistance of C.A. Ávila-Herrera and M.A. Hernández-Landaverde, the use of LIDTRA facilities and the support of CONACYT-Mexico (Project numbers 242549 and 271031) are gratefully acknowledged.

References

1. S. Ru. *Sol. Energy*. 130 (2016) 139.
2. H.A. Mohamed. *Sol. Energy*. 108 (2014) 360.
3. J. Hernández-Borja, Y. V. Vorobiev, R. Ramírez-Bon. *Sol. Energy Mater. Sol. Cells*. 95 (2011) 1882.
4. K.P. Bhandari, P.J. Roland, H. Mahabaduge, N.O. Haugen, C.R. Grice, S. Jeong, T. Dykstra, J. Gao, R.J. Ellingson. *Energy Mater. Sol. Cells*. 117 (2013) 476.
5. R.A. Orozco-Terán, M. Sotelo-Lerma, R. Ramírez-Bon, M.A. Quevedo-López, O. Mendoza- *Thin Solid Films*. 343–344 (1999) 587.
6. J.J. Valenzuela-Jáuregui, R. Ramírez-Bon, A. Mendoza-Galván, M. Sotelo-Lerma. *Thin Solid Films*. 441 (2003) 104.
7. I.E. Morales-Fernández, M.I. Medina-Montes, L.A. González, B. Gnade, M.A. Quevedo-López, R. Ramírez-Bon. *Thin Solid Films*. 519 (2010) 512.
8. M.B. Ortuño López, J.J. Valenzuela-Jáuregui, M. Sotelo-Lerma, A. Mendoza-Galván, R. Ramírez-Bon. *Thin Solid Films*. 429 (2003) 34.
9. M.G. Sandoval-Paz, M. Sotelo-Lerma, Mendoza-Galvan, R. Ramírez-Bon. *Thin Solid Films*. 515 (2007) 3356.
10. I.R. Chávez-Urbiola, J.A. Bernal Martínez, J. Hernández Borja, C.E. Pérez García, R. Ramírez-Bon, Y. V. Vorobiev. *Energy Procedia*. 57 (2014) 24.
11. A. Hussain, H. Shanjit, A. Rahman. *Superlattices Microstruct.* 89 (2016) 43.
12. F. Göde, E. Güneri, F.M. Emen, V. Emir Kafadar, S. Ünlü. *J. Lumin.* 147 (2014) 41.
13. A.S. Obaid, M.A. Mahdi, Z. Hassan, M. Bououdina. *Mater. Sci. Semicond. Process.* 15 (2012) 564.
14. S. Rajathi, K. Kirubavathi, K. Selvaraju. *Arab. J. Chem.* (2014).
15. J. Ji, H. Ji, J. Wang, X. Zheng, J. Lai, W. Liu, T. Li, Y. Ma, H. Li, S. Zhao, Z. Jin. *Thin Solid Films*. 590 (2015) 124.
16. E. Yücel, Y. Yücel, B. Beleli. *J. Alloys Compd.* 642 (2015) 63.
17. I.R. Chávez Urbiola, J.A. Bernal Martínez, V.P. Makhniy, R. Ramírez Bon, Y. V. Vorobiev., *Inorg. Mater.* 50 (2014) 546.
18. S. Meraz-Dávila, I.R. Chávez-Urbiola, C.E. Pérez García, A. Sánchez-Martínez, S.A. Campos-Montiel, C.G. Alvarado-Beltrán, Y. V. Vorobiev, R. Ramírez-Bon. *Int. J. Electrochem. Sci.* 11 (2016) 2962.
19. A.M. Selman, Z. Hassan. *Sensors Actuators A Phys.* 221 (2015) 15.
20. R.R. Salunkhe, D.S. Dhawale, D.P. Dubal, C.D. Lokhande. *Sensors Actuators B Chem.* 140 (2009) 86.
21. A.S. Kamble, R.C. Pawar, J.Y. Patil, S.S. Suryavanshi. *J. Alloys Compd.* 509 (2011) 1035.
22. A.M. Selman, Z. Hassan. *Mater. Res. Bull.* 73 (2016) 29.
23. R.R. Salunkhe, C.D. Lokhande. *Sensors Actuators, B Chem.* 129 (2008) 345.
24. A. Hendi. *J. Alloys Compd.* 647 (2015) 259.
25. S.K. Singh, P. Hazra, S. Tripathi, P. Chakrabarti. *Superlattices Microstruct.* 91 (2016) 62.
26. D.L. Pulfrey, G. Parish, D. Wee, B.D. Nener. *Solid. State. Electron.* 49 (2005) 1969.
27. F. Yakuphanoglu, F.S. Shokr, R.K. Gupta, A. a. Al-Ghamdi, S. Bin-Omran, Y. Al-Turki, F. El-Tantawy. *J. Alloys Compd.* 650 (2015) 671.
28. K. Yong, H. Kang, W. Lee, C. Lee, J. Park, H. Sung, S. Im, H. Kim, S. Kim, B. Min, H. Kim, *Mater. Sci. Semicond. Process.* 33 (2015) 154.
29. A.M. Selman, Z. Hassan, M. Husham, N.M. Ahmed. *Appl. Surf. Sci.* 305 (2014) 445..
30. K.Y. Ko, H. Kang, J. Kim, W. Lee, H.S. Lee, S. Im, J.Y. Kang, J.-M. Myoung, H.-G. Kim, S.-H. Kim, H. Kim. *Mater. Sci. Semicond. Process.* 27 (2014) 297.
31. Z. Yuan, Y. Ren. *Phys. E Low-Dimensional Syst. Nanostructures.* 48 (2013) 128.
32. B. Arredondo, B. Romero, J. Pena, A. Fernández-Pacheco, E. Alonso, R. Vergaz, C. de Dios.

- Sensors*. 13 (2013) 12266.
33. K.J. Baeg, M. Binda, D. Natali, M. Caironi, Y.-Y. Noh. *Adv. Mater.* 25 (2013) 4267.
34. T. Rauch, M. Böberl, S.F. Tedde, J. Fürst, M. V. Kovalenko, G. Hesser, U. Lemmer, W. Heiss, O. Hayden. *Nat. Photonics*. 3 (2009) 332.
35. M.A.B. Kenneth W. Busch, *Multielement Detection Systems for Spectrochemical Analysis*, 1990.
36. F. Alema, B. Hertog, O. Ledyae, D. Volovik, R. Miller, A. Osinsky, S. Bakhshi, W. V. Schoenfeld. *Sensors Actuators A Phys.* 249 (2016) 263.
37. Z. Yuan and Y. Ren. *Phys. E Low-Dimensional Syst. Nanostructures* 48 (2013) 128.
38. Arredondo, B. Romero, J. Pena, A. Fernández-Pacheco, E. Alonso, R. Vergaz, and C. de Dios. *Sensors*. 13 (2013) 12266.
39. K. J. Baeg, M. Binda, D. Natali, M. Caironi, and Y.-Y. Noh. *Adv. Mater.* 25 (2013) 4267.
40. T. Rauch, M. Böberl, S. F. Tedde, J. Fürst, M. V. Kovalenko, G. Hesser, U. Lemmer, W. Heiss, and O. Hayden. *Nat. Photonics* 3 (2009) 332.
41. T. P. Osedach, S. M. Geyer, J. C. Ho, A. C. Arango, M. G. Bawendi, and V. Bulović. *Appl. Phys. Lett.* 94 (2009) 43307.
42. P. E. Keivanidis, S.-H. Khong, P. K. H. Ho, N. C. Greenham, and R. H. Friend. *Appl. Phys. Lett.* 94 (2009) 17330.
43. Tatar, D. Demiroglu, and M. Urgan. *Microelectron. Eng.* 126 (2014) 184.
44. M. A. B. Kenneth W. Busch, *Multielement Detection Systems for Spectrochemical Analysis*. 1990.
45. F. Alema, B. Hertog, O. Ledyae, D. Volovik, R. Miller, A. Osinsky, S. Bakhshi, and W. V. Schoenfeld. *Sensors Actuators A Phys.* 249 (2016) 263.

© 2018 The Authors. Published by ESG (www.electrochemsci.org). This article is an open access article distributed under the terms and conditions of the Creative Commons Attribution license (<http://creativecommons.org/licenses/by/4.0/>).